JOURNAL OF PROPULSION AND POWER
Vol. 13, No. 3, May–June 1997

Antiproton Catalyzed Fusion Propulsion for Interplanetary Missions

B. N. Cassenti*
United Technologies Research Center, East Hartford, Connecticut 06084
and
T. Kammash† and D. L. Galbraith‡
University of Michigan, Ann Arbor, Michigan 48109

Interplanetary trips using chemical propellants require years to complete. A recently completed study on an antiproton catalyzed fusion reaction propulsion system has shown that the specific impulses that can be obtained are between 1500 s for a contained system to over 100,000 s for a system that directly uses the fusion reaction products. Thrust-to-weight ratios exceeding 1 can be sustained. This allows considerably shorter solar system travel times than conventional chemical propellants. Missions considered range from inner to outer solar system distances. A tradeoff can be made between reducing travel time and reducing initial mass in low Earth orbit. Missions to the inner planets can be shortened considerably for a given mass ratio, whereas missions to the outermost planets will be several weeks in duration.

Nomenclature

A = atomic weight
$\bar{B}$ = steady magnetic field strength
$\dot{B}$ = rate of increase of magnetic field strength
C_p = primary (longitudinal) wave speed
d = spot diameter
E = Young's modulus
E_f = energy in fission fragments
E_α = alpha particle energy
E_π = pion energy
g = acceleration of gravity
I_{sp} = specific impulse
k = Boltzmann's constant
MR = mass ratio
m_{amu} = atomic mass unit
m_f = mass of fusion fuel
m_T = total pellet mass
N = number of alpha particles
R_c = core radius
s = distance traveled through pellet core
T = temperature
t = time
v_e = exhaust velocity
x = distance traveled
Z = atomic number
α = angle between temperature gradient and electron density gradient
Δv = change in speed
ε = recoil energy
ν = Poisson ratio
ν_f = number of fission neutrons
ν_π = number of pions
ρ = mass density
ρ_w = tungsten density
$\langle \sigma v \rangle$ = fusion reaction rate
ϕ_i = launch angle

Received June 28, 1996; presented as Paper 96-3068 at the AIAA/ASME/SAE/ASEE 32nd Joint Propulsion Conference, Lake Buena Vista, FL, July 1–3, 1996; revision received Jan. 19, 1997; accepted for publication Feb. 19, 1997.

*Senior Principal Engineer, Materials and Structures. Associate Fellow AIAA.
†Professor, Department of Nuclear Engineering and Radiological Sciences.
‡Adjunct Faculty, Department of Nuclear Engineering and Radiological Sciences.

Introduction

DURING the last decade antiproton annihilation propulsion has been the subject of considerable research.[1–5] The use of antiprotons to directly heat a propellent requires at least milligrams of antimatter to perform useful missions.[6] Milligram quantities of antiprotons are well beyond current capabilities and will require substantial technological improvements before becoming a reality.[7,8] Concepts for using antiprotons to catalyze fusion reactions that would require far fewer antiprotons have recently been proposed.[9–13] The approaches are based on 1) antiproton fissioning of heavy nuclei,[10–12] 2) direct antiproton heating for igniting a fusion reaction,[9,13] and 3) muon production using antiprotons for muon catalyzed fusion.[14]

The Lewis et al.[10–12] proposal to use antiprotons to fission heavy nuclei has been the subject of considerable research. When an antiproton annihilates in a heavy nucleus of uranium or plutonium, the nucleus fissions 100% of the time.[15,16] More than 20% of the fission energy is present in the fission fragments and over one dozen neutrons are emitted. Some of these neutrons initially released will produce additional fissions with a considerably lower yield of neutrons. The energy present in the fission fragments is readily absorbed by the fusion fuel, but it is difficult to absorb the neutron kinetic energy, and the absorption of the gamma ray energy is extremely difficult. Nevertheless, antiproton annihilation provides a means for sustaining fission reactions without a critical mass of fissionable material. The fission energy then provides a means for initiating fusion reactions.

Shamatov[13] Cassenti,[5,17] Kammash and Galbraith,[9] and Howe and Metzger[18] have proposed using the annihilation of antiprotons (or antihydrogen) to initiate fusion reactions directly. When an antiproton annihilates in matter it produces mostly pions and about 5% kaons. About 60% of the pions are charged. The pions are moving at relativistic velocities (about 95% of the speed of light), and the absorption of the kinetic energy requires on the order of meters of path length

for significant energy absorption. Of course, the energy must be absorbed before the pions decay (i.e., in about 20 ns) into a muon and an associated neutrino. The muons are charged and will travel on the order of kilometers before decaying. The muon has a mean life about 100 times the life of a pion. Because muons are charged, they can also deposit energy in the plasma. The muon decays into an electron, or a positron, and two associated neutrinos. The electrons, or positrons, can also deposit energy in a plasma. To increase the path length in the plasma, a magnetic field could be applied, but the relativistic speeds require extremely large fields. For example, about 100 kG are required for a 1-m-diam containment and 10 MG for a 1-cm-diam pellet. Magnetic fields are difficult to generate in a steady state, but can be generated in transient situations. Hasegawa[19] and Kammash and Galbraith[20,21] have proposed using magnetic fields developed at the surface of laser-heated materials. At the heated surface the material is ionized, with the ion cores and the electrons sharing the absorbed energy. The ions and electrons stream away from the surface with the electrons moving faster than the ion cores. The ions and electrons moving into the surface are readily stopped. Hence, there is a net negative current flow away from the surface. The net current flow creates a magnetic field that readily contains the plasma. Measurements and models[22–24] indicate that the fields are large enough to contain the annihilation products resulting when an antiproton annihilates on a nucleus, and the field is large enough to isolate the plasma from a surrounding heavy metal shell. The shell will contain the plasma because of its strength and inertia, in a manner similar to inertial confinement fusion. The antiprotons provide a lightweight mechanism for heating the plasma to fusion ignition temperatures, and, hence, are well suited for use in propulsion systems.

The last method proposed for using antiprotons as a catalyst to initiate fusion reactions uses the muons, resulting from antiproton–nucleon annihilations, to sustain muon-catalyzed fusion of a deutrium–tritium mixture.[14] The antiprotons provide a compact source for the muons when compared to the accelerators that have been proposed[25] and, hence, are ideal for use in propulsion systems.

Each of the cited methods for using antiprotons to catalyze fusion reactions present disadvantages for use in propulsion. Pellet designs for antiproton-catalyzed fission reactions require an initial compression using ion beams.[11,12] The ion accelerators are heavy and there would be a distinct advantage in eliminating them. Direct heating of the plasma to initiate a fusion reaction uses very little of the annihilation energy, about 2% (Ref. 9). Muon-catalyzed fusion is effective in a narrow temperature range, at about 1200 K to support a resonance between the tritium and deuterium atoms in a molecule. These low temperatures will be difficult to sustain.

This paper will use a combination of antiproton-induced fission and magnetically insulated inertial confinement fusion.[25] Muon catalyzed fission could be utilized by injecting muons, from an antiproton annihilation, at appropriately heated points in the fusion fuel, at the correct time.

Fusion pellets are ideal for use in nuclear pulse propulsion systems. Over the last four decades nuclear pulse propulsion has been proposed in several forms.[26–29]

Parlos and Metzger[29] have recently shown that a 100-ton nuclear device can be contained by a 9.4-m-radius vessel, 0.2 m thick. The inside of the vessel wall would be lined with molybdenum. Each detonation would ablate about 0.3 cm of molybdenum. The final thickness of the molybdenum would have to be about 1 cm for optimum performance. The vessel wall itself would consist of stainless steel reinforced with NICALON fibers. The vessel would have a mass of about 1800 metric tons. When the vessel was charged with hydrogen at 1 atm, the specific impulse was about 1000 s and the thrust-to-mass ratio was about 2. The predictions of Parlos and Metzger[29] were obtained using results from previous numerical simulations. Although these simulations are an aid in scaling, they do not allow a complete examination of the relative merits of various approaches.

A simple model has been developed[30] that allows investigators to estimate various effects and predict the performance of a contained system. Estimates from this simple model predicted a higher performance than the simulations used by Parlos and Metzger,[29] but are still somewhat below the ideal performance (i.e., the performance without losses). The simple model was built from several models. These included a model of the expansion of the gas from the blast, a model of the structural response of the chamber, a model of the heating of the containment chamber wall, and a performance model for the performance of the rocket.

Propulsion Model Summary

The propulsion system to be considered is a nuclear pulse system. Such systems make use of nuclear explosions (fission or fusion) to propel a vehicle. The basic design problem is to reduce the size of the nuclear devices which, of course, would require a subcritical mass of uranium or plutonium. Such devices would satisfy the theory banning the use of nuclear weapons in space. These pellet-size devices need to make use of as many effects as possible to reduce their size. In this section we illustrate such a device, which makes use of several observed effects.

The pellet to be ignited consists of several materials. The fusion fuel can be deuterium–tritium, or lithium deuteride.[31] The fuel has an outer radius R_f and an inner radius R_c (see Fig. 1). The fuel contains a hemisphere of fissionable material such as U^{235}, U^{238}, and Pu^{239}. The fusion fuel is surrounded by a shell consisting of a heavy metal. The outer layer of the shell should be a dense high-melting temperature material such as tungsten. The inside shell layer can be a neutron generating or reflecting material, such as uranium. The shell and fuel have a hole of diameter d, which is perpendicular to the flat surface of the hemisphere of fissionable material. The flat surface of the hemisphere is assumed to be a small distance δ below the surface.

A pulse of antiprotons and positrons[13] is injected through the hole in the shell. The energy of the antiprotons is chosen so that the annihilation occurs at the surface of the hemisphere. The annihilation of the antiprotons ionizes the fuel above the hemisphere. Fuel ions fill the empty core of the pellet with a plasma. The electrons created by the annihilation create a current flow developing a transient magnetic field. The field is contained within the shell and traps charged particles (fission fragments, ion cores, electrons, muons, and pions). The charged particles heat the core of the pellet to fusion temperatures. The uranium on the inside layer of the shell generates and/or reflects some neutrons back into the fuel, whereas the tungsten shell contains the fusion fuel hopefully long enough for the fusion reaction to go to completion.

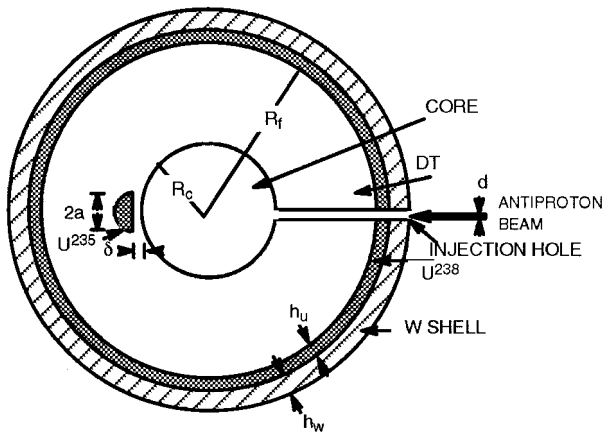

Fig. 1 Pellet construction and geometry (from Ref. 25).

The pulse of antimatter should consist of equal quantities of antiprotons and positrons to preserve neutrality.[13] The pulse can be antihydrogen or it can be partially or completely ionized. Sodium beams have been focused to nanometer spots using lasers.[32] This provides a limit on achievable spot sizes.

The annihilation of the antiprotons will ionize material in the immediate neighborhood and release relativistic particles. The nonuniform heating will create magnetic fields that can be roughly estimated as[22]

$$\frac{1}{1\ \text{MG}}\dot{B} = \frac{1}{10\ \text{ps}}\left(\frac{T}{1\ \text{keV}}\right)\left(\frac{10\ \mu\text{m}}{d}\right)^2 \sin\alpha \tag{1}$$

$$\frac{1}{1\ \text{MG}}\bar{B} = 3.6\left(\frac{T}{1\ \text{keV}}\right)^{1/2}\left(\frac{10\ \mu\text{m}}{d}\right)\left[\frac{A^{1/2}(Z+1)^{-1/2}}{1.1}\right]\sin\alpha \tag{2}$$

where $\dot{B}$ is the rate of change of the magnetic field in megagauss, with respect to time, $\bar{B}$ is the steady magnetic field, A is the atomic weight of the plasma (taken to be 2.5 for deuterium–tritium fuel), and Z is the atomic number of the plasma. α is the angle between the gradient in the electron density and the electron temperature gradient. To transition between the growth, Eq. (1) and the steady field, Eq. (2), we can take the transient field $B(t)$ to be

$$B(t) = \bar{B}(1 - e^{-\nu t}) \tag{3}$$

where

$$\nu = \frac{\dot{B}}{\bar{B}} = \frac{1}{36\ \text{ps}}\left(\frac{T}{1\ \text{keV}}\right)^{1/2}\left(\frac{10\ \mu\text{m}}{d}\right)\left[\frac{1.1}{A^{1/2}(Z+1)^{-1/2}}\right] \tag{4}$$

at $t = 0$.

Equations (1–4) do not depend on the electron density directly, but only on the ratio of the electron density gradient and the electron density. This leaves only a length scale. The previous equations are used to describe the transient magnetic field.

The pions developed in an annihilation will deposit a small portion of their energy in the plasma, before they leave the pellet. The energy deposition $\mathrm{d}E/\mathrm{d}x$ will be on the order of

$$\frac{\mathrm{d}E}{\mathrm{d}x} \approx 0.5\ \frac{\text{MeV}}{\text{cm}}\left(\frac{\rho_{\text{plasma}}}{\rho_{\text{LH}_2}}\right) \tag{5}$$

where $\rho_{\text{plasma}}/\rho_{\text{LH}_2}$ is the ratio of the plasma density to the density of liquid hydrogen. There will also be a recoil energy for annihilations in the plasma ε of about 20 MeV (Ref. 9).

The path length over which the energy is deposited is given by

$$s \approx 2R_c \tag{6}$$

if the path is helical because of the presence of a magnetic field.

The energy E_π deposited by the pions and the recoil ε is

$$E_\pi = \frac{1}{2}\nu_\pi\frac{\mathrm{d}E}{\mathrm{d}x}s + \varepsilon \tag{7}$$

where ν_π is the number of charged pions created at the annihilation site (about 3.6). If the magnetic fields develop slowly, the pions will move through the core with a distance of R_c instead of $2Rc$.

One-half of the pions move into pellet core with the plasma and the other half move into the fission hemisphere.

When the antiproton annihilates on the flat of the hemisphere, the material will fission releasing the kinetic energy of fission fragments E_f and a number of neutrons and pions, which can cause additional fissions; from Ref. 12 for U^{238}

$$\nu_f \approx 13.7 \tag{8}$$

$$E_f \approx 170\ \text{MeV} \tag{9}$$

Half of the released neutrons will enter the fission hemisphere and can cause additional fissions. These additional fissions have been shown to have little effect on the performance[31] and will be neglected. The energy deposited in the core, per antiproton annihilation, is now given by summing Eqs. (7) and (9). Multiplying by the number of antiprotons gives the total energy deposited. Only the mass of pellet between the core and the uranium hemisphere is heated. We take this mass to be the plasma density in the core times the volume of the core.

The magnetic fields decay sufficiently slowly to contain the plasma pressure until the fusion reaction begins. The confinement time t_i is certainly greater than the time for a p-wave to propagate through the thickness of the tungsten shell.[19]

The p-wave speed in a solid is given by

$$C_p = \sqrt{\frac{(1-\nu)E}{(1+\nu)(1-2\nu)\rho_w}} \tag{10}$$

where E is about 4.1×10^{12} dyne/cm^2 for room temperature tungsten and ν is about 0.23 for room-temperature tungsten. The inertial confinement time is bounded by

$$t_i > (h_w/C_p) \tag{11}$$

Actually, the inertial confinement times will be much greater than the time for a p-wave to propagate through the thickness of the shell. An integration of the elastic–plastic equations of motion for the tungsten shell was performed to find the time for the tungsten radius to double. The equations of motion are given in Ref. 31. The magnetic fields acted for a time sufficient to confine the plasma in the core.

A rough calculation indicates that heating of the tungsten shell (e.g., because of fission gamma-ray emission) will not raise the shell temperature by more than 100°C. Hence, room-temperature properties can be used. Recall that the magnetic fields will insulate the shell from the plasma.

The inertial confinement time t_f must be greater than the time for the plasma to fuse,[19] where

$$t_f = \frac{6\ \text{kT}}{E_\alpha n_{\text{plasma}}\langle\sigma v\rangle} \tag{12}$$

where T is the plasma temperature, and n_{plasma} is the plasma number density.

An upper limit on the plasma temperature and the core energy can be found from

$$\tfrac{3}{2}NkT = \tfrac{1}{2}NE_\alpha \tag{13}$$

The ideal specific impulse of the system can now be determined by assuming all of the fusion alpha particle energy, from all of the fuel, is emitted with the total mass of the pellet. The v_e can then be determined from

$$\frac{1}{2}m_T v_e^2 = \frac{m_f E_\alpha}{2Am_{\text{amu}}} \tag{14}$$

The I_{sp} can then be approximated as

$$I_{\text{sp}} = v_e/g \tag{15}$$

The model can now be used to examine specific pellet designs.

The previous model was used to predict the response of typical pellet.[31] A deuterium–tritium fuel was taken for simplicity. The alpha particle energy produced in a fusion reaction was taken to be 3.5 MeV (Ref. 18). This was the energy assumed to be present in the exhaust, since the alpha particle can be directed by magnetic fields. The $\langle \sigma v \rangle$ was taken to be 10^{-15} cm^3/s, which occurs at a plasma temperature of 80 keV.

The description and dimensions (in centimeters), respectively, of a typical pellet geometry are as follows: core radius R_f, 0.005; fuel radius R_c, 1.0; uranium shell thickness h_u, 0.0; tungsten shell thickness h_w, 0.01; antiproton beam radius d, 0.00001; uranium hemisphere radius α, 0.003; and hemisphere distance from core surface δ, 0.0055. The pellet has a shell of tungsten 0.01 cm thick and there is no uranium on the inside of the shell. The shell has as outer radius of about 1 cm. The hemisphere of uranium is so small that secondary fissions account for 0.08% of the energy released. The antimatter pulse contains 2×10^{13} antiprotons and lasts 30 ns. The core density is about 1.00×10^{21}/cm^3, only if the material above the flat uranium surface enters the core. The core temperature is 85 keV. The magnetic field reaches about 24 MG at end of the pulse. The tungsten shell does not move during the heating by the antimatter pulse. The characteristic inertial confinement time is at least 4 μs and the time for the fusion reaction is about 150 ns. The total mass of the pellet is about 3.5 g and absorbs about 7.3×10^{17} erg, producing a specific impulse of about 600,000 s for complete (100%) fusion burning. If 10% of the fuel fuses, the ideal specific impulse is about 200,000 s, whereas 5% yields about 150,000 s for an ideal specific impulse. If the pellet is used in a contained system to heat hydrogen propellant, then the specific impulse will be between 2700–3700 s (Ref. 30), depending on the propellent and ablated mass with a thrust-to-mass ratio of about 30.

The pellet geometry was summarized previously. Of course, if the pellet is scaled to the size of a thermonuclear warhead, then, with some variations in design, a single antiproton (or neutron) will trigger the critical mass fission device, resulting in nearly complete fusion. Hence, if the pellet is scaled up in size (and designed as in a thermonuclear warhead) then the pellet will ignite and fuse. The design problem is how to shrink the pellet to sizes on the order of 1 cm. If the pellets do not contain a critical mass of uranium or plutonium then the propulsion system will not violate the space nuclear weapon ban.

Other variations in the design are also possible. The hole in the shell and the fuel can be removed (i.e., filled) with the antiproton energy tuned to pass through the shell and fuel and then annihilate at the fissionable hemisphere.[33] The tritium can be replaced with Li^6 (the lithium will make the tritium upon absorbing a neutron), which will eliminate the radioactive hazard of tritium[1] and the need for a cryogenic system. Finally, plastic can be used to absorb gamma rays (i.e., x rays) as in a thermonuclear warhead.[34] Certainly, if the pellets were the size of a thermonuclear warhead, both the L_i^6 and the plastic become effective.

Interplanetary Trajectory Models

Estimates for the performance of various propulsion systems can be readily obtained using the equations of celestial mechanics. There are several excellent texts that can provide the necessary background for completing performance calculations (e.g., Ref. 35).

In our celestial mechanics-based models we have assumed that all maneuvers are impulse maneuvers. Hence, the time to change the velocity is much shorter than the total transit time for the mission. This is true for lower specific impulse fusion rockets (about 3000 s), but may not hold when the specific impulse is near the limit for fusion propulsion (about 1,000,000 s). All of the planets will be assumed to be orbiting the sun in circular orbits with all of the orbits in the same plane. Finally, no use will be made of aeroassists or gravity assists.

The trajectory consists of 1) the departure from Earth orbit, 2) the transit to the planet, and 3) the insertion into a low orbit about the planet. The return trip is assumed to have the same energy requirements as the Earth departure trip. Hence, only the trajectory to the planet needs to be examined. This means that the stay time at the planet could be a significant fraction of a year. The Earth departure orbit and the parking orbit about the planet are both assumed to be at an altitude equal to the radius of the planet. Two types of missions will be considered: 1) minimum energy transfer (Hohmann transfer) and 2) a minimum time transfer for a given target mass ratio.

Rocket Performance

Using the previous assumptions the performance of the fusion rocket can be represented by I_{sp}. The rocket equation then leads to the following relation between MR and Δv:

$$MR = \exp(\Delta v / I_{sp} g_0) \tag{16}$$

where g_0 is the acceleration of gravity at the Earth's surface, and MR is defined as the ratio of the initial mass to the final mass.

Hohmann Trajectories

Hohmann minimum energy trajectories for interplanetary transits are well known and its parameters can be readily calculated.[35]

The speed changes at the Earth and the planet can be found from 1) the Hohmann transfer ellipse speeds at aphelion and perihelion, 2) the speeds of the planets, and 3) the circular orbit speeds about the Earth and the planet. The total change in speed can now be used to find the mass ratio for various values of the specific impulse. Finally, the total transit time is just half the orbital period of the Hohmann transfer ellipse.

The solar system data used for the evaluation are summarized in Appendix A, and was taken from Ref. 36. The transit times are given as follows, and, of course, do not depend on the specific impulse. The Hohmann minimum energy transfer time; the planet and time (in years) are, respectively, Mercury, 0.289; Venus, 0.400; Mars, 0.713; Vesta, 1.085; Ceres, 1.293;

Table 1 Hohmann trajectory mass ratio I_{sp} (s)

Planet	500	1000	3000	10,000	30,000	100,000	150,000	200,000	600,000
Mercury	14.430	3.799	1.560	1.143	1.045	1.013	1.009	1.007	1.002
Venus	3.719	1.929	1.245	1.068	1.022	1.007	1.004	1.003	1.001
Mars	3.061	1.750	1.205	1.058	1.019	1.006	1.004	1.003	1.001
Vesta	5.815	2.411	1.341	1.092	1.030	1.010	1.006	1.004	1.001
Ceres	6.736	2.595	1.374	1.100	1.032	1.009	1.006	1.005	1.002
Jupiter	97.77	9.888	2.146	1.258	1.079	1.023	1.015	1.012	1.003
Saturn	33.50	5.788	1.795	1.192	1.060	1.018	1.012	1.009	1.003
Uranus	18.25	4.272	1.623	1.156	1.050	1.015	1.010	1.007	1.002
Neptune	21.03	4.586	1.611	1.164	1.052	1.015	1.010	1.008	1.003
Pluto	10.33	3.215	1.476	1.124	1.040	1.012	1.008	1.006	1.002

Jupiter, 2.731; Saturn, 6.048; Uranus, 16.04; Neptune, 30.59; and Pluto, 45.61. The mass ratio required for various values of the specific impulse are given in Table 1. It can be seen that the mass ratios become approximately unity for values of the specific impulse of 30,000 s or more.

Minimum Transfer Time Trajectories

The trip times, though are quite large for trips to the outer solar system. Consuming more fuel could greatly reduce the trip time. Here the trip time will be minimized for a chosen mass ratio. Throughout this paper this mass ratio was taken to be 1.5. Note from Table 1 that this eliminates values for the specific impulse of less than 1000 s for all of the planets listed; even for a specific impulse of 3000 s many missions cannot be completed. In Table 1 all maneuvers were assumed to be impulsive.

As in the case of the Hohmann trajectories, the minimum time trajectories can be modeled in three parts: 1) the departure from Earth orbit, 2) the transit to the planet, and 3) the insertion into orbit about the planet. Figure 2 illustrates the geometry for the departure from Earth orbit. There are two parameters that will determine the trip time to the planet: they are the velocity increment added to the circular orbit velocity, which is given by Eq. (18), and by ϕ_i. We have assumed that the impulse is applied tangent to the direction of motion. The launch angle is bounded by

$$-\pi < \phi_i < \pi \tag{17}$$

and the change in velocity Δv_i, and must be less than the total change in speed that is given by Eq. (16), that is,

$$\Delta v_i = f I_{sp} g_0 \ell n\, MR \tag{18}$$

where the factor f must be less than 1. The minimum transit time was found by incrementing through the range for the launch angle, and the velocity factor f to find the trajectories that reach the target planet. The trajectory with minimum travel time was found and tabulated. Appendix B summarizes the equations used in the model.

Figures 3 and 4 illustrate the results of the analysis. For values of the specific impulse on the order of 500,000 s, the trip times to Mars are on the order of one day, trips to Mercury and Venus (Fig. 3) will still require a few days, and trips to the asteroid belt will be several days. Hence, even for very high values of the specific impulse, fusion rockets trip times to the inner planets will be longer than typical trip times around the Earth now. For trips to the outer planets (Fig. 4) trip times are never less than one week for high specific impulse fusion rockets, and trips to Pluto will be about one-half year. Hence, it will be helpful to make use of aeroassists and gravity assists whenever possible.

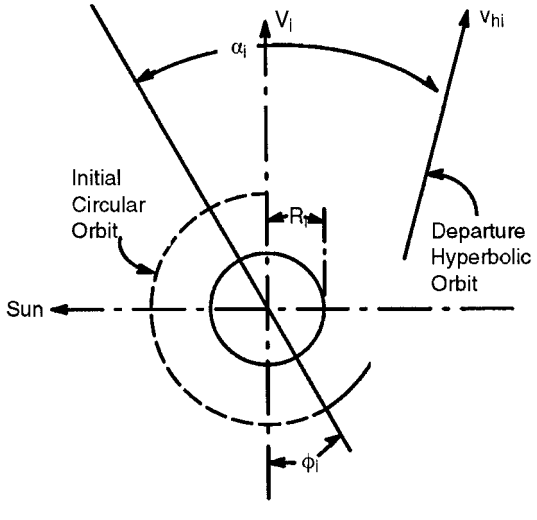

Fig. 2 Earth departure orbit.

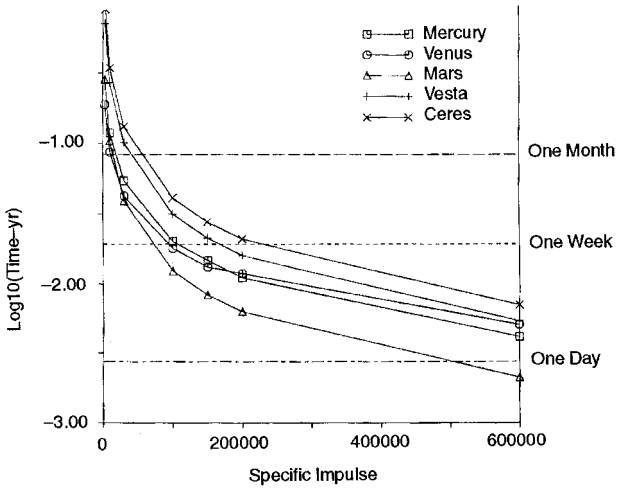

Fig. 3 Minimum transit time for a mass ratio of 1.5 to the inner planets.

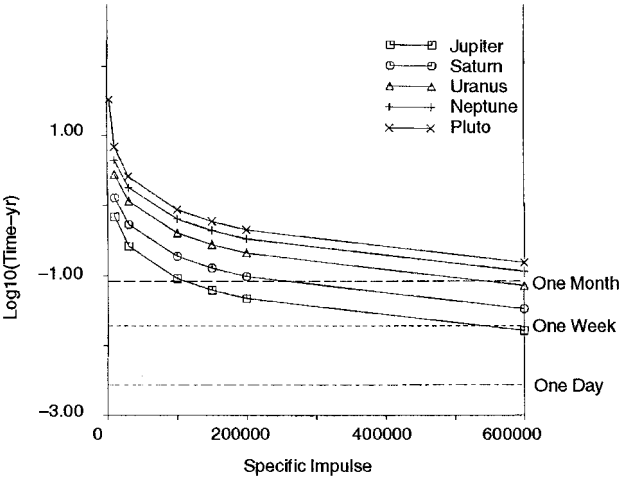

Fig. 4 Minimum transit time for a mass ratio of 1.5 to the outer planets.

Conclusions

Inertial confinement fusion rockets can significantly increase the specific impulse over current values for chemical, solid, and gas core nuclear fission rockets. The performance increase will open up the solar system to settlement and trade, but the trip times to the outer solar system will be too long for quick trips to the outer solar system without making use of additional assists.

Appendix A: Solar System Parameters

The characteristic solar system constants used in the evaluation of the orbits were Re = 6.378E06 m for the radius of the Earth, au = 1.496E11 m for the astronomical unit, yr = 31.557E06 s for the length of the year, MO = 1.989E30 kg for the mass of the sun, Me = 5.976E24 kg for the mass of the Earth, g_0 = 9.80665 m/s for the acceleration of gravity, and G = 6.67259E-11 Nm/kg for the gravitational constant.

The data used for the planets are in Table A1.[36]

Appendix B: Solar Transit Orbit Model

The total available speed change is given by

$$\Delta v = I_{sp} g_0 \ell n\, MR \tag{B1}$$

Table A1 Data used for the planets

Planet	Mass, *Me*	Radius, *Re*	Distance, *au*
Mercury	0.0553	0.382	0.3871
Venus	0.8149	0.949	0.7233
Earth	1.0000	1.000	1.0000
Mars	0.1074	0.532	1.5327
Vesta	0.000022	0.039	2.352
Ceres	0.000134	0.0717	2.767
Jupiter	317.938	11.209	5.2028
Saturn	95.181	9.449	9.5388
Uranus	14.531	4.007	19.1914
Neptune	17.135	3.883	30.0511
Pluto	0.0022	0.180	39.5294

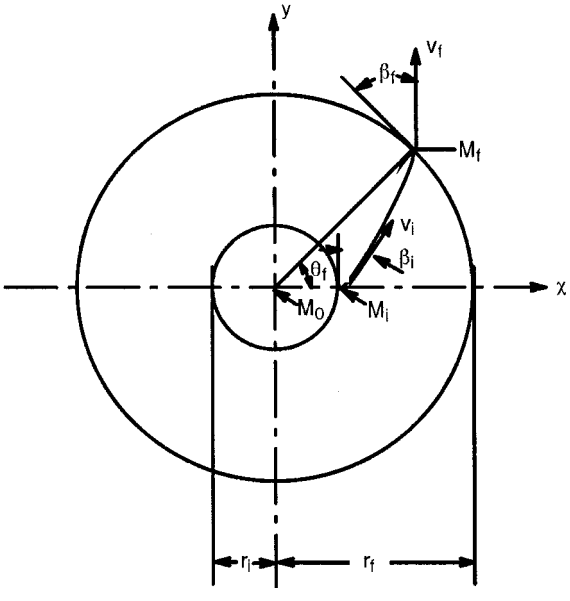

Fig. B1 Solar transit orbit parameters.

The initial speed change from the circular orbit about Earth to the hyperbolic escape orbit is a fraction f of the total available speed change or

$$\Delta v_i = f\Delta v \tag{B2}$$

where $0 \leq f \leq 1$.

The fraction f and the launch angle ϕ_i in Fig. 1 (which is bounded by $-\pi \leq \phi_i \leq \pi$), are incremented over the available range.

The departure orbit can now be found

$$v_{pi} = \Delta v_i + \sqrt{GM_i/R_i} \tag{B3}$$

is the perigee velocity

$$E_i = \tfrac{1}{2} v_{pi}^2 - (GM_i/R_i) \tag{B4}$$

is the specific energy

$$v_{hi} = \sqrt{2E_i} \tag{B5}$$

is the hyperbolic excess velocity

$$h_i = v_{pi}R_i \tag{B6}$$

is the specific angular momentum

$$P_i = h_i^2/GM_i \tag{B7}$$

is the semiparameter

$$e_i = \sqrt{1 - (P_i/\alpha_i)} \tag{B8}$$

is the eccentricity

$$\alpha_i = \cos^{-1}(1/e_i) \tag{B9}$$

is the departure angle.

The solar transfer orbit can now be evaluated (see Fig. B1)

$$v_i = \sqrt{v_{hi}^2 + V_i^2 + 2V_i v_{hi}\cos(\alpha_i - \phi_i)} \tag{B10}$$

is the initial solar orbit velocity, where

$$V_i = \sqrt{GM_i/r_i} \tag{B11}$$

is the Earth orbit velocity

$$\beta_i = \tan^{-1}\left[\frac{v_{hi}\sin(\alpha_i - \phi_i)}{V_i + v_{hi}\cos(\alpha_i - \phi_i)}\right] \tag{B12}$$

is the departure angle

$$E_0 = \tfrac{1}{2} v_i^2 - (GM_0/r_i) \tag{B13}$$

is the specific energy

$$\alpha_0 = -(GM_0/2E_0) \tag{B14}$$

is the semimajor axis

$$h_0 = r_i v_i \cos\beta_i \tag{B15}$$

is the specific angular momentum

$$e_0 = \sqrt{1 - (p_0/\alpha_0)} \tag{B16}$$

is the eccentricity

$$v_f = \sqrt{2[E_0 + (GM_0/r_f)]} \tag{B17}$$

is the final solar velocity

$$\theta_0 = \cos^{-1}\{(1/e_0)[(p_0/r_i) - 1]\} \tag{B18}$$

is the perihelion location

$$\theta_f = \theta_0 + \cos^{-1}\{(1/e_0)[(p_0/r_f) - 1]\} \tag{B19}$$

is the final angular location

$$B_f = \cos^{-1}(h_0/r_f v_f) \tag{B20}$$

The arrival orbit parameters can now be found

$$v_{hf} = \sqrt{v_f^2 + V_f^2 - 2v_f V_f \cos\beta_f} \tag{B21}$$

where

$$v_f = \sqrt{GM_f/R_f} \tag{B22}$$

is the hyperbolic excess velocity

$$E_f = \tfrac{1}{2} v_{hf}^2 \tag{B23}$$

is the specific energy

$$v_{pf} = \sqrt{2[E_f + (GM_f/R_f)]} \tag{B24}$$

is the periapsis velocity

$$\Delta v_f = v_{pf} - \sqrt{GM_f/R_f} \tag{B25}$$

is the change in speed to go onto the circular parking orbit the total $\Delta v_i + \Delta v_f$ can now be compared to Δv in Eq. (B1). Values of f and β_i can now be found by interpolation.

Finally, the transit time can now be evaluated by using any standard method of celestial mechanics.

References

[1]Forward, R. L., "Antiproton Annihilation Propulsion," *Journal of Propulsion and Power*, Vol. 1, No. 5, 1985, pp. 370–374.

[2]Morgan, D. L., "Investigation of Matter — Antimatter Interactions for Possible Propulsion Applications," NASA CR-141356, Jan. 1975.

[3]Vulpetti, G., "Antimatter Propulsion for Space Exploration," AIAA Paper 85-491, Oct. 1985.

[4]Howe, S. D., and Metzger, J. D., "Survey of Antiproton-Based Propulsion Concepts and Potential Impact on a Manned Mars Mission," Los Alamos National Lab., LA-UR-87-2191, Los Alamos, NM, 1987.

[5]Cassenti, B. N., "Conceptual Designs for Antiproton Space Propulsion Systems," *Journal of Propulsion and Power*, Vol. 7, No. 3, 1991, pp. 368–373.

[6]Cassenti, B. N., "Antimatter Propulsion for OTV Applications," *Journal of Propulsion and Power*, Vol. 1, No. 2, 1985, pp. 143–149.

[7]Cassenti, B., Mannheim, P., and Gould, P., "Concepts for the Efficient Production and Storage of Antimatter," AIAA Paper 93-2031, July 1993.

[8]Cassenti, B. N., "Concepts for the Efficient Production of Antimatter," *11th Symposium on Space Nuclear Power and Propulsion*, American Inst. of Physics, Albuqurque, NM, 1994, pp. 1429–1434.

[9]Kammash, T., and Galbraith, D. L., "Antimatter-Driven-Fusion Propulsion for Solar System Exploration," *Journal of Propulsion and Power*, Vol. 8, No. 3, 1992, pp. 644–649.

[10]Lewis, R. A., Smith, G. A., Kanzlecter, R. J., and Newton, R., "Antiproton Based Microfusion," *Fusion Technology*, Vol. 20, Dec. 1991, pp. 1046–1050.

[11]Lewis, R. A., Smith, G. A., Kanzlecter, R. J., and Newton, R., "An Antiproton Driver for Internal Confinement Fusion Propulsion," AIAA Paper 91-3618, Sept. 1991.

[12]Lewis, R. A., Smith, G. A., Toothacker, W. S., and Kanzlecter, R. J., "An Antiproton Catalyst for Internal Confinement Fusion Propulsion," AIAA Paper 90-2760, July 1990.

[13]Shmatov, M. L., "Ignition of Thermonuclear Microexplosions with Antimatter," A.F.IOFFE Physical Technical Inst., Academy of Sciences of Russia, Preprint 1621, St. Petersburg, Russia, 1993.

[14]Takahashi, H., "Thoughts on the Muon Catalyzed Fusion Process for Antimatter Propulsion and for the Production of High Mass Number Nuclei," *Antiproton Science and Technology*, edited by B. W. Augenstein, B. E. Bonner, F. E. Mills, and M. M. Nieto, World Scientific, Singapore, 1988, pp. 603–619.

[15]Morgan, D. L., "Annihilation of Antiprotons in Heavy Nuclei," U.S. Air Force Rocket Propulsion Lab., TR 86-011, Edwards AFB, CA, Oct. 1986.

[16]"Antiproton Induced Fission in 238U and 209Bi," *Physics at LEAR with Low Energy Antiprotons, Proceedings of the Fourth Low Energy Antiproton Ring Workshop*, Villars-sur-Ollon, Switzerland, PS 177 Collaboration, 1988, pp. 793–796.

[17]Cassenti, B. N., "High Specific Impulse Antimatter Rockets," AIAA Paper 91-2548, June 1991.

[18]Howe, S., and Metzer, J., "Antiproton Based Propulsion Concepts and Potential Impact on a Manned Mars Mission," *Journal of Propulsion and Power*, Vol. 5, No. 3, 1989, pp. 295–300.

[19]Hasegawa, A., "Magnetically Insulated Inertial Confinement Fusion: A New Approach to Controlled Thermonuclear Fusion," *Physical Review Letters*, Vol. 56, No. 2, 1986, pp. 139–142.

[20]Karmmash, T., and Galbraith, D. L., "A High Gain Fusion Reactor Based on the Magnetically Insulated Inertial Confinement Fusion (MICF) Concept," *Nuclear Fusion*, Vol. 29, No. 7, 1989, pp. 1079–1099.

[21]Kammash, T., and Galbraith, D. L., "Reaction Physics and Mission Capabilities of the MICF Reactor," *Journal of Propulsion and Power*, Vol. 6, No. 4, 1990, pp. 412–415.

[22]Sakagani, Y., "Two Dimensional Distribution of Self-Generated Magnetic Fields near the Laser Plasma Resonant Interaction Region," *Physical Review Letters*, Vol. 42, No. 13, 1979, pp. 839–842.

[23]Max, C. E., Manheimer, W. M., and Thomson, J. J., "Enhanced Transport Across Laser Generated Magnetic Fields," *Physics of Fluids*, Vol. 21, No. 1, 1978, pp. 128–139.

[24]Raven, A., Willi, O., and Rumsby, P. T., "Megagauss Magnetic Field Profiles in Laser Produced Plasmas," *Physical Review Letters*, Vol. 41, No. 8, 1978, pp. 554–557.

[25]Subotowics, M., "Propulsion Concepts for Nuclear Matter Compression Energy and 'Cold' Fusion Energy Sources in Interstellar Flight," *Acta Astronautica*, Vol. 17, No. 8, 1988, pp. 937–942.

[26]Nance, J. P., "Nuclear Pulse Propulsion," *IEEE Transactions on Nuclear Science*, Vol. NS-12, No. 1, 1965, pp. 177–182.

[27]Martin, A. R., and Bond, A., "Nuclear Pulse Propulsion: A Historical Review of an Advanced Propulsion Concept," *Journal of the British Interplanetary Society*, Vol. 32, 1979, pp. 283–310.

[28]Solem, J. D., "Medusa: Nuclear Explosive Propulsion for Interplanetary Travel," *Journal of the British Interplanetary Society*, Vol. 46, No. 1, 1993, pp. 21–26.

[29]Parlos, A. G., and Metzger, J. D., "Feasibility Study of a Contained Pulsed Nuclear Propulsion Engine," *Journal of Propulsion and Power*, Vol. 10, No. 2, 1994, pp. 269–278.

[30]Cassenti, B. N., "A Contained Antiproton Catalyzed Pulse Nuclear Propulsion System," AIAA Paper 95-2898, July 1995.

[31]Cassenti, B. N., Rammash, T., and Golbraith, D. L., "An Antiproton Catalyzed Inertial Fusion Propulsion System," edited by T. Kammash, Vol. 167, Progress in Astronautics and Aeronautics, AIAA, Washington, DC, 1995, pp. 75–88.

[32]Timp, G., Behringer, R. E., Tennant, D. M., Cunningham, J. E., Prentis, M., and Bergen, K. K., "Using Light as a Lens for Submicron Neutral-Atom Lithography," *Physical Review Letters*, Vol. 69, No. 11, 1992, pp. 1636–1639.

[33]Morgan, D. L., Jr., "Annihilation Localization in Gas-Core and Plasma Core Annihilation Rocket Engines," 39th Congress of the International Astronautical Federation, Paper 88-554, Washington, DC, Oct. 1988.

[34]Rhodes, R., *The Making of the Atomic Bomb*, Simon and Schuster, New York, 1986, pp. 774–776.

[35]Bate, R. R., Mueller, D. D., and White, J. E., *Fundamentals of Astrodynamics*, Dover, New York, 1971.

[36]Beatty, J. K., and Charkin, A. (eds.), *The New Solar System*, 3rd ed., Cambridge Univ. Press, New York, 1990.